C. P. No. 594

C. P. No. 594

MINISTRY OF AVIATION

AERONAUTICAL RESEARCH COUNCIL

CURRENT PAPERS

Measurements of the Pitching Moment Derivatives for Rigid Wings of Rectangular Plan Form Oscillating about the Mid-Chord Axis in Supersonic Flow

By

C. Scruton, B.Sc., L. Woodgate,
K. C. Lapworth, M.Sc., Ph.D.,
and J. F. M. Maybrey

of the Aerodynamics Division, N. P. L.

LONDON: HER MAJESTY'S STATIONERY OFFICE

1962

PRICE 3s. 6d. NET

C.P. No.594

Measurements of the Pitching Moment Derivatives for Rigid Wings of Rectangular Plan Form Oscillating about the Mid-Chord Axis in Supersonic Flow

- By -
C. Scruton, B.Sc., L. Woodgate,
K. C. Lapworth, M.Sc., Ph.D.,
and J. F. M. Maybrey
of the Aerodynamics Division, N.P.L.

March, 1961

SUMMARY

Pitching moment derivatives have been measured by a free oscillation technique on wings of rectangular planform and of double wedge section with a thickness/chord ratio of 0·12. The wings of aspect ratio 1, 2, 3, 4 and 5 were oscillated about the half-chord axis in flows of Mach number 1·79, 2·15 and 2·43. The Reynolds number and frequency parameter of the tests were less than 10^6 and 0·03 respectively. Tunnel boundary-layer effects were avoided by the use of a reflection plate. The influence of a body (non-oscillating) with various nose shapes was also investigated.

On the plain wings it was found that the general trend of the variation with aspect ratio was predicted by theory but the numerical values differed considerably. The presence of a body tended to reduce the value of the damping derivative.

---

1. Introduction

A previous report[1] describes measurements of pitching moment derivatives made on aerofoils oscillating in two-dimensional supersonic flow. The present report describes a continuation of these tests with finite wings to determine the influence of aspect ratio, and to provide experimental data for comparison with calculated derivatives. The influence of the proximity of a body (non-oscillating) with various nose shapes was also investigated.

The measurements were made by the free oscillation method using a half-span model mounted on a reflection plate to by-pass the tunnel boundary layer. The length of the body used in the tests was limited by the size of the reflection plate, and this size was fixed by considerations of the interference of the flow over the model by disturbances from the leading edges of the plate after reflection from the tunnel walls. These limitations were most severe at the lower Mach numbers and necessitated a compromise between length of body and the lowest test Mach number. The model proportions adopted are shown in Fig. 1 and were suitable in the 14 in. × 11 in. working section wind tunnel used for Mach numbers above 1·7. A few of the tests were repeated with the reflection plate removed and the model mounted on the tunnel wall.

The/

Previously issued as A.R.C.22,682,
Published with the permission of the Director, National Physical Laboratory.

The wings tested were all of rectangular planform and were of double-wedge section with a thickness/chord ratio of 0·12 and the aspect ratio was varied from 1·0 to 5·0. Tests were made at Mach numbers of 1·79, 2·15 and 2·43, the Reynolds numbers of the tests ranging from $0{\cdot}86 \times 10^6$ to $0{\cdot}62 \times 10^6$. For all the tests the wings oscillated in pitch about the half-chord axis with a frequency parameter of about 0·02.

2. Notation

M Mach number

V wind speed

ρ air density

c wing chord

s wing semi-span. For the present purpose this is taken to be the distance between the outboard and inboard edges of the model half-wing, and does not include the body radius

$A.R. = \dfrac{2s}{c}$, aspect ratio

I moment of inertia of oscillating system

σ elastic stiffness coefficient of oscillating system

K apparatus damping coefficient

$-M_\theta$ aerodynamic stiffness derivative

$-m_\theta = \dfrac{-M_\theta}{\rho V^2 c^2 s}$, non-dimensional form of $-M_\theta$

$-M_{\dot\theta}$ aerodynamic damping derivative

$-m_{\dot\theta} = \dfrac{-M_{\dot\theta}}{\rho V c^3 s}$, non-dimensional form of $-M_{\dot\theta}$

f frequency of oscillation

$\omega = 2\pi f$, angular frequency

δ logarithmic decrement of oscillation (natural logarithm of the ratio of the amplitude of successive cycles of oscillation).

θ angular displacement in pitching motion (radians)

Suffix o applied to the quantities f, ω and δ denotes the values assumed by these quantities for tests in vacuo.

3. Basic Formulae

The aerodynamic moment acting on the aerofoil is written

$$\mathcal{M} = M_\theta \theta + M_{\dot\theta} \dot\theta$$

and for simple harmonic motions of frequency $\omega/2\pi$, $\mathcal{M}$ is expressed in terms of its non-dimensional in-phase and out-of-phase components as

$\mathcal{M}$/

$$\mathcal{M} = \rho V^2 c^2 s(m_\theta + i\nu m_{\dot\theta})\theta$$

where $\nu = \omega c/V$.

The equation of motion of the aerofoil performing free oscillations in pitching motion against a spring constraint is then

$$I\ddot\theta + (K - M_{\dot\theta})\dot\theta + (\sigma - M_\theta)\theta = 0.$$

On substitution of the solution

$$\theta = \theta_o e^{\mu t} \sin\omega t$$

and assuming, as was found in the experiments, that $\mu^2 - \mu_o^2 \ll \omega^2 - \omega_o^2$ and $\mu_o^2 \ll \omega_o^2$, the following expressions for $-M_\theta$ and $-M_{\dot\theta}$ are found*

$$-M_\theta = \frac{\sigma}{f_o^2}(f - f_o)(f + f_o)$$

$$-M_{\dot\theta} = 2I(f\delta - f_o\delta_o)$$

where the suffix o denotes quantities measured in vacuo.

4. Description of Apparatus

The wind tunnel

The tests were carried out in the N.P.L. continuous flow supersonic wind tunnel which was fitted with a working section of height 14 in. and width 11 in. The tunnel stagnation pressure could be reduced from one atmosphere to about one-quarter of an atmosphere. The tunnel humidity was controlled by introducing dry air both before and during the run, the surplus air being extracted by pumps. Humidity effects were avoided by only testing at frost points of -15°F or lower.*

The model mountings

Use was made of one of the two mountings used previously for the tests on two-dimensional aerofoils spanning the tunnel. The arrangement is shown diagrammatically in Fig. 2 and a photograph of the mounting is reproduced as Fig. 3.

The oscillating system was mounted on a rigid bracket fixed to the tunnel wall and consisted essentially of a cylinder suspended on two sets of cross-spring bearings and a torque bar to provide the required stiffness against rotation of the cylinder. The inner end of the cylinder terminated in a circular plate to which another circular plate with a flange for attaching the model wing, was fitted concentrically. The model wing after passing through the rectangular hole in the reflection plate and the rectangular tube which connected the reflection plate to the air-tight box, was attached to the flange on the outer circular plate. For the body proximity tests the half-cylindrical body, which had a specially shaped hole to allow the wing to pass through it, was fixed directly to the reflection plate as were the interchangeable body noses. The box and its connections to the reflection plate were made as air-tight as possible to prevent air leakage into the tunnel over the model wing from either the outside of the tunnel or from the space behind the reflection plate. The

system/

---

* This criterion was the result of an investigation carried out in the previous tests[1].

system was made to oscillate by means of a spring loaded plunger which operated against an arm fixed to the rotating cylinder.

The models

The 12% thick double-wedge model used for the previous two-dimensional tests was cut to provide a rectangular wing of aspect ratio 5. This model was successively cropped to give aspect ratios of 4, 3, 2 and 1. (Note that to facilitate the comparison of results in the body proximity tests the aspect ratio is defined as the total wing span less the body diameter, divided by the chord.) The diameter of the cylindrical body was made equal to the chord of the wing, so that the A.R.5 wing became the A.R.4 wing for body proximity tests and so on.

The measuring and recording equipment

The electronic equipment was the same as used in the previous tests and is fully described in that report[1]. Briefly the system consisted of a simple condenser gauge, which, used in conjunction with the Southern Instruments F.M. equipment produced a D.C. voltage proportional to the angular displacement of the model. This voltage was displayed on one beam of a double-beam oscilloscope; the other beam was fed with time pulses at 0·01 sec intervals. A film record was made by photographing the screen with a continuously moving film camera, and this record was analysed in a specially designed optical viewer which allowed the peak to peak amplitude of individual cycles and the frequency of the oscillation to be readily measured. The logarithmic decrement was then determined in the usual way.

5. Method of Test

The logarithmic decrement and the frequency were determined as described in the previous paragraph. The elastic stiffness was obtained by a static experiment and the values of the apparatus damping and the *in vacuo* moment of inertia of the system were obtained from free oscillation tests carried out with the tunnel evacuated to about $\frac{1}{4}$ atmospheric pressure. This was the minimum pressure attainable.

6. Results

As in the previous tests the value of the damping derivative $-m_{\dot{\theta}}$ was found to be generally dependent on the amplitude θ but very little variation with amplitude of the value of the stiffness derivative $-m_{\theta}$ was observed. All the experimental results are tabulated (Tables 1 to 5) but the values of $-m_{\dot{\theta}}$ which are plotted refer to a standard amplitude of $\theta = 0{\cdot}01$ rads. The results for plain wings are plotted against aspect ratio and against Mach number in Figs. 4, 5 and 6 and the results for the body proximity tests are plotted in Figs. 7 and 8. The values of $-m_{\dot{\theta}}$, and to a lesser extent those of $-m_{\theta}$, measured at $M = 1{\cdot}79$ and $M = 2{\cdot}15$ on the plain wing of A.R.5 and at $M = 1{\cdot}79$ on A.R.4 wing do not conform to the general trend indicated by theory (Fig. 6). Various explanations for this based on shock wave interference on the tip of the wing were examined but none of these can be substantiated from the geometry of the tunnel and the reflection plate. A possible explanation is that the wind load, which would be a maximum in these cases, might have been sufficient to deflect some part of the oscillatory system to cause slight friction. It was unfortunate that these results were not confirmed before the aspect ratio of the model was reduced.

The values of the damping and stiffness derivatives ($-m_{\dot{\theta}}$ and $-m_{\theta}$) were small, as would be expected for the mid-chord axis position. The actual change in damping and frequency between the 'wind on' and 'in vacuo' conditions to be measured was less than in the corresponding two-dimensional tests

because/

because of the smaller wing area and, as the aspect ratio decreased, the amount to be measured became progressively less. The accuracy of measurement was therefore not very high but it was sufficient to demonstrate the general trends and to show that there was no very large change in the derivatives due to the flow over the tip of the wing.

7. Discussion of Results

(a) Plain wing tests (Figs. 4, 5 and 6)

The experimental results are compared with the values obtained by Acum's modification of Van Dyke's theory to rectangular wings[2]. The values of the derivatives are numerically larger than those predicted but they conform to the general trends indicated by theory. A similar result was found in the two-dimensional tests[1], the results of which are also shown on the plots of Figs. 4, 5 and 6. For the larger aspect ratios the experimental and the theoretical values differ by about the same amount as was found in the two-dimensional tests.

(b) Body proximity tests (Figs. 7 and 8)

The derivative values obtained with the body present showed considerable scatter, especially with the lower aspect ratio wings, and it is therefore difficult to assess the trends due to changes of the nose shape.

As might be expected, the influence of the body was most marked with the low aspect ratio wings, substantial reductions in the value of the damping derivative $-m_{\dot{\theta}}$ being obtained when the body was present.

(c) Comparison of results obtained with model on tunnel wall and with model on reflection plate

Measurements with the model mounted on the tunnel wall were made with wings of aspect ratio 1 and 2 only. The differences between the values thus obtained and those obtained using a reflection plate were most marked with the wing of A.R.1 (Table 1). These tests were carried out with the body present whereas those with the A.R.2 wing were made with the plain wing. It should be noted however that the distance between the wing tip and the reflection plate was the same for the A.R.2 plain wing and the A.R.1 wing with body. Similarly the distance between the wing tip and the tunnel wall was the same for the tests with the model mounted directly on the tunnel wall. The differences found with the A.R.1 wing may, therefore, have been due to the inaccuracies of the measurements on the low aspect ratio wings.

Conclusions

1. For the plain wings the trends of variation of the derivatives with aspect ratio are predicted by Acum's[2] modified Van Dyke theory but the numerical values differ considerably.

2. The presence of a body tends to reduce the value of the aerodynamic damping $-m_{\dot{\theta}}$. The reduction is most marked at the lower aspect ratios.

3. The accuracy of the data obtained does not permit the influence of the shape of the nose of the body to be determined.

References/

References

No.	Author(s)	Title, etc.
1	C. Scruton, L. Woodgate, K. C. Lapworth and J. Maybrey	Measurement of pitching moment derivatives for aerofoils oscillating in two-dimensional supersonic flow. A.R.C. R. & M.3234. January, 1959.
2	W. E. A. Acum	Note on the effect of thickness and aspect ratio on the damping of pitching oscillations of rectangular wings moving at supersonic speeds. A.R.C. C.P.151. May, 1953.

Table 1/

Table 1

Results for Aspect Ratio 1

Nose Type	M	Experiment					Theory	
		ν	θ_c	$-m_\theta$	$-m_{\dot\theta}$	$\theta_c=0{\cdot}01$ $-m_{\dot\theta}$	$-m_\theta$	$-m_{\dot\theta}$
On Reflection Plate								
None	1·79	0·021	0·018 0·010 0·005	-0·18	0·23 0·43 0·70	0·43	-0·175	0·149
Ogival	1·79	0·021		-0·22	0·11	0·11		
15° Cone	1·79	0·021		-0·21	0·11	0·11		
30° Cone	1·79	0·021		-0·20	0·22	0·22		
45° Cone	1·79	0·021		-0·20	0·13	0·13		
On Tunnel Wall								
15° Cone	1·79	0·021	0·019 0·007	-0·27	0·19 0·24	0·22		
45° Cone	1·79	0·021		-0·27	0·17	0·17		
On Reflection Plate								
None	2·15	0·019	0·016 0·005	-0·14	0·22 0·16	0·19	-0·131	0·105
Ogival	2·15	0·019		-0·15	0·08	0·08		
15° Cone	2·15	0·019	0·018 0·006	-0·15	0·07 0·04	0·05		
30° Cone	2·15	0·019		-0·14	0·08	0·08		
45° Cone	2·15	0·019		-0·23	0·19	0·19		
On Reflection Plate								
None	2·43	0·018		-0·13	0·23	0·23	-0·114	0·087
Ogival	2·43	0·018	0·015 0·004	-0·21	0·17 0·05	0·12		
15° Cone	2·43	0·018		-0·19	0·17	0·17		
30° Cone	2·43	0·018	0·018 0·005	-0·16	0·09 0·07	0·08		
45° Cone	2·43	0·018	0·019 0·005	-0·14	0·11 0·05	0·07		

Table 2/

Table 2

Results for Aspect Ratio 2

Nose Type	M	Experiment					Theory	
		ν	θ_c	$-m_\theta$	$-m_{\dot\theta}$	$-m_{\dot\theta}$ $\theta_c=0{\cdot}01$	$-m_\theta$	$-m_{\dot\theta}$
On Reflection Plate								
None	1·79	0·021	0·015 0·013 0·004	-0·17	0·23 0·20 0·11	0·20	-0·137	0·112
Ogival	1·79	0·021	0·015 0·014 0·006 0·005	-0·16	0·14 0·13 0·10 0·07	0·11		
15° Cone	1·79	0·021	0·016 0·006	-0·15	0·14 0·10	0·12		
30° Cone	1·79	0·021		-0·15	0·16	0·16		
45° Cone	1·79	0·021		-0·16	0·17	0·17		
On Tunnel Wall								
None	1·79	0·021		-0·17	0·18	0·18		
On Reflection Plate								
None	2·15	0·019		-0·15	0·16	0·16	-0·107	0·087
Ogival	2·15	0·019	0·012 0·004	-0·13	0·09 0·05	0·08		
15° Cone	2·15	0·019		-0·14	0·08	0·08		
30° Cone	2·15	0·019		-0·15	0·09	0·09		
45° Cone	2·15	0·019		-0·12	0·10	0·10		
On Reflection Plate								
None	2·43	0·018		-0·15	0·17	0·17	-0·097	0·075
Ogival	2·43	0·018	0·014 0·004	-0·12	0·11 0·09	0·10		
15° Cone	2·43	0·018		-0·12	0·08	0·08		
30° Cone	2·43	0·018		-0·15	0·09	0·09		
45° Cone	2·43	0·018	0·012 0·004	-0·14	0·11 0·10	0·11		
On Tunnel Wall								
None	2·43	0·018	0·014 0·004	-0·13	0·15 0·09	0·13		

Table 3/

Table 3

Results for Aspect Ratio 3

Nose Type	M	Experiment					Theory	
		ν	θ_c	$-m_\theta$	$-m_{\dot\theta}$	$\theta_c=0{\cdot}01$ $-m_{\dot\theta}$	$-m_\theta$	$-m_{\dot\theta}$
On Reflection Plate								
None	1·79	0·021	0·015 0·005	−0·15	0·18 0·20	0·19	−0·124	0·100
Ogival	1·79	0·021		−0·17	0·14	0·14		
15° Cone	1·79	0·021		−0·16	0·15	0·15		
30° Cone	1·79	0·021	0·019 0·011	−0·16	0·029 0·014	0·012		
45° Cone	1·79	0·021		−0·17	0·09	0·09		
On Reflection Plate								
None	2·15	0·019	0·013 0·003	−0·14	0·12 0·20	0·15	−0·100	0·081
Ogival	2·15	0·019		−0·13	0·12	0·12		
15° Cone	2·15	0·019	0·015 0·005	−0·14	0·10 0·13	0·12		
30° Cone	2·15	0·019	0·020 0·015	−0·13	0·08 0·10	0·13		
45° Cone	2·15	0·019		−0·14	0·11	0·11		
On Reflection Plate								
None	2·43	0·018		−0·14	0·16	0·16	−0·091	0·071
Ogival	2·43	0·018		−0·13	0·11	0·11		
15° Cone	2·43	0·018	0·015 0·005	−0·13	0·11 0·09	0·10		
30° Cone	2·43	0·018		−0·12	0·10	0·10		
45° Cone	2·43	0·018	0·015 0·005	−0·11	0·10 0·12	0·11		

Table 4/

Table 4

Results for Aspect Ratio 4

Nose Type	M	Experiment					Theory	
		ν	θ_c	$-m_\theta$	$-m_{\dot\theta}$	$-m_{\dot\theta}$ $\theta_c=0{\cdot}01$	$-m_\theta$	$-m_{\dot\theta}$
On Reflection Plate								
None	1·79	0·21	0·018 0·010 0·005	-0·19	0·20 0·28 0·32	0·28	-0·118	0·094
Ogival	1·79	0·21		-0·15	0·13	0·13		
15° Cone	1·79	0·21		-0·16	0·13	0·13		
30° Cone	1·79	0·21		-0·14	0·11	0·11		
45° Cone	1·79	0·21	0·025 0·010		0·15 0·14	0·14		
On Reflection Plate								
None	2·15	0·19		-0·15	0·16	0·16	-0·096	0·078
Ogival	2·15	0·19	0·020 0·005	-0·15	0·13 0·15	0·14		
15° Cone	2·15	0·19	0·020 0·005	-0·15	0·13 0·15	0·14		
30° Cone	2·15	0·19		-0·14	0·16	0·16		
45° Cone	2·15	0·19		-0·13	0·12	0·12		
On Reflection Plate								
None	2·43	0·18		-0·14	0·13	0·13	-0·088	0·069
Ogival	2·43	0·18	0·015 0·007	-0·13	0·12 0·11	0·11		
15° Cone	2·43	0·18		-0·16	0·14	0·14		
30° Cone	2·43	0·18	0·015 0·003	-0·13	0·14 0·12	0·13		
45° Cone	2·43	0·18	0·015 0·007	-0·13	0·12 0·11	0·11		

Table 5/

Table 5

Results for Aspect Ratio 5

Tests with this aspect ratio were made only without the body.

Nose Type	M	Experiment					Theory	
		ν	θ_c	$-m_\theta$	$-m_{\dot\theta}$	$-m_{\dot\theta}$ at $\theta_c=0{\cdot}01$	$-m_\theta$	$-m_{\dot\theta}$
On Reflection Plate								
None	1·79	0·021	0·016 0·007 0·004	-0·22	0·30 0·24 0·20	0·26	-0·114	0·091
None	2·15	0·019		-0·17	0·22	0·22	-0·093	0·076
None	2·43	0·018	0·012 0·004	-0·13	0·15 0·13	0·14	-0·087	0·068

ES

FIG. 1

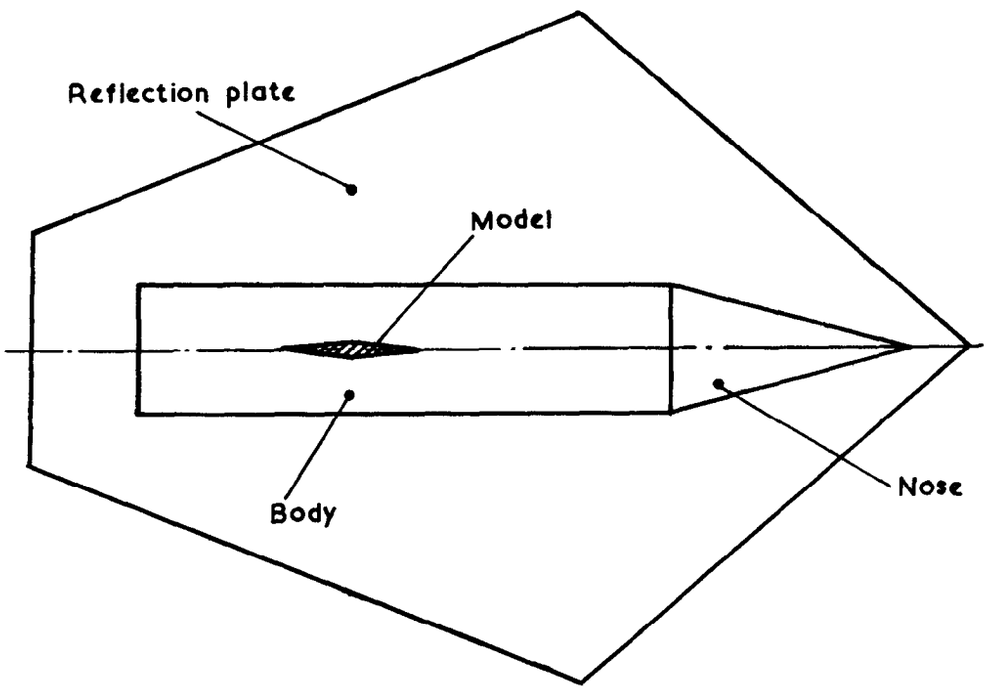

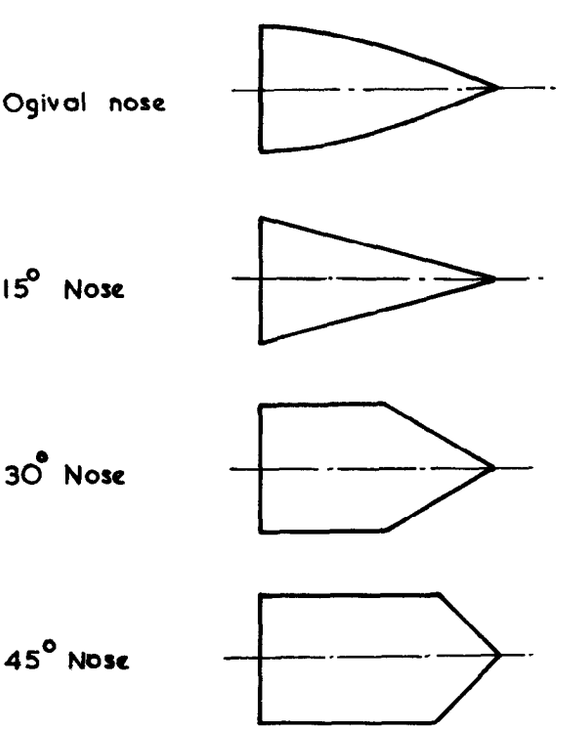

General arrangement of body and wing on the reflection plate.

FIG. 2.

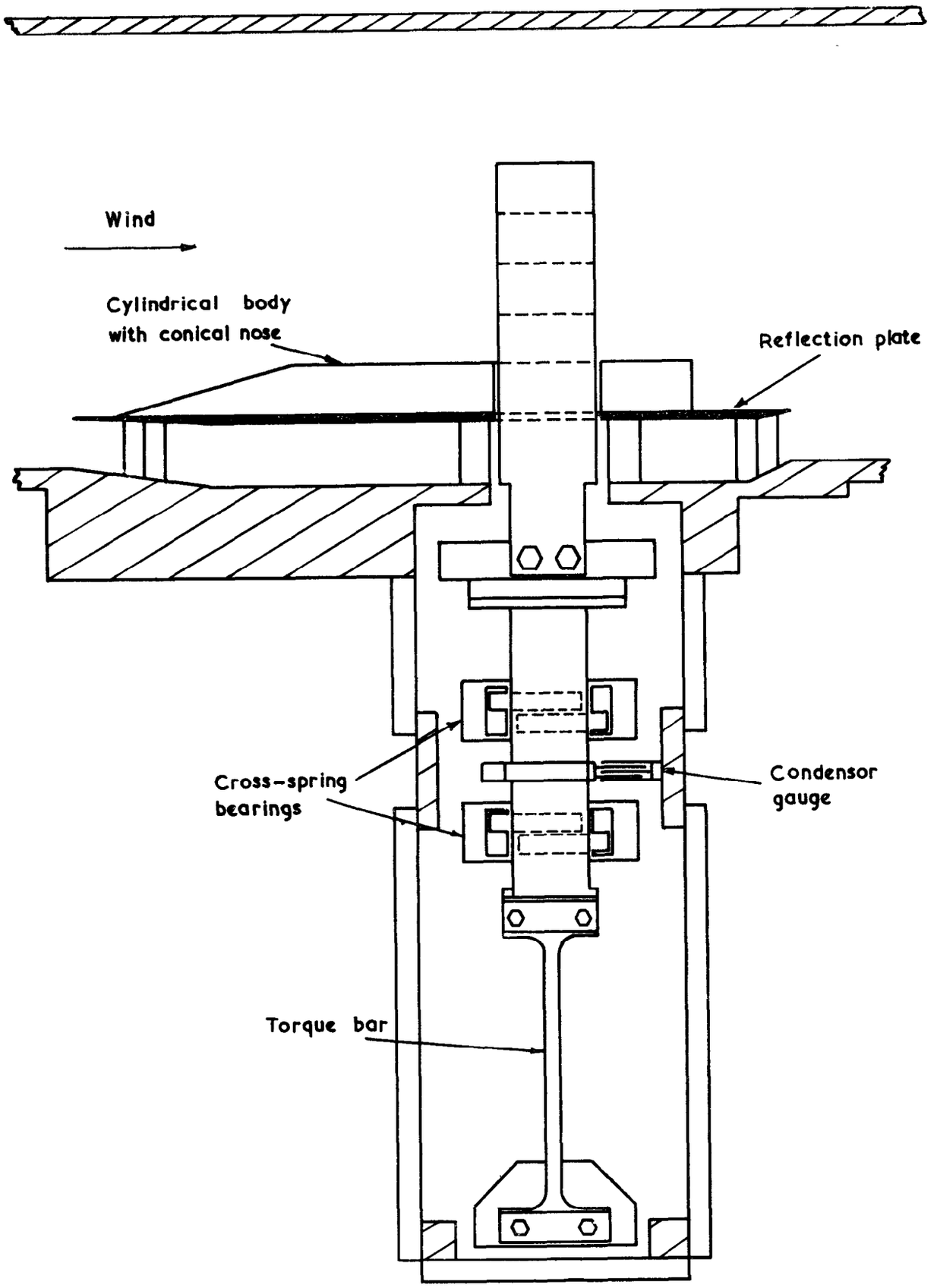

General arrangement of model & spring bearing (plan view).

FIG. 3.

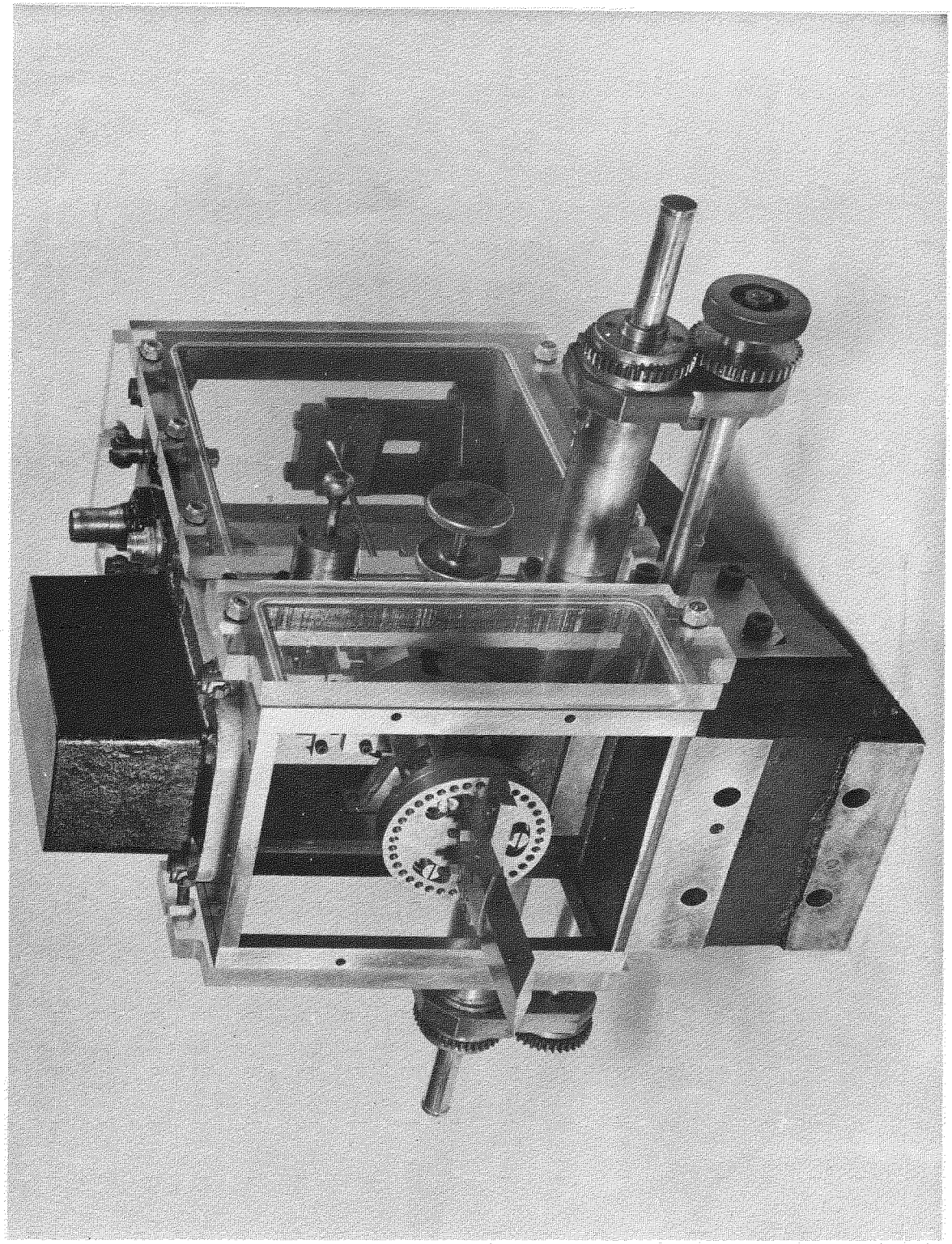

Photograph of model mounting.

FIG. 4.

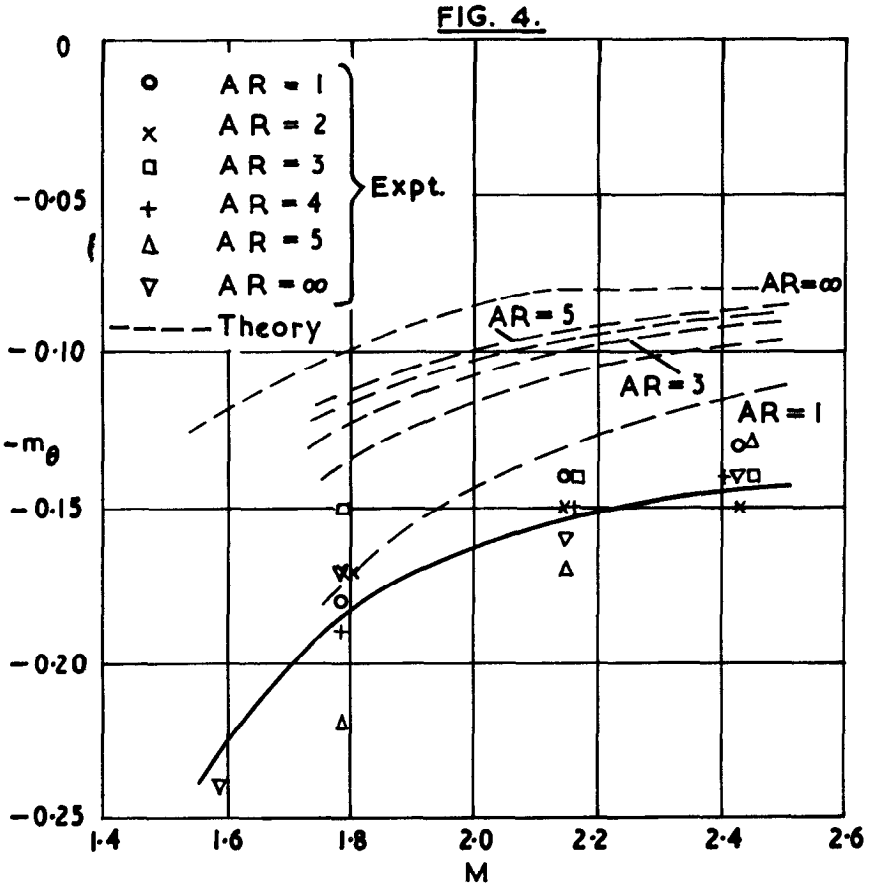

Variation of $-m_\theta$ with Mach number for the plain wings.

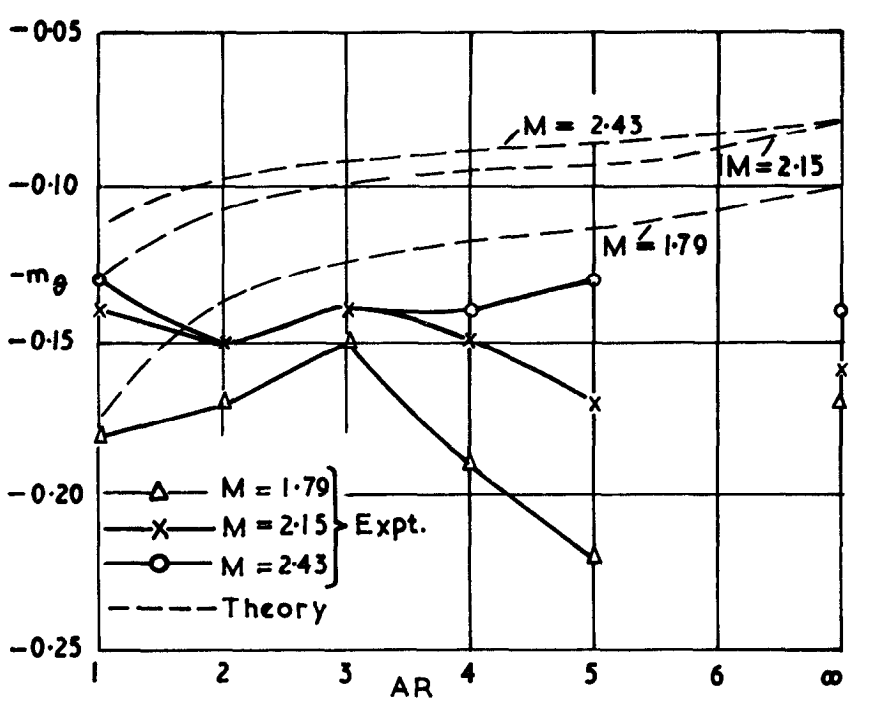

Variation of $-m_\theta$ with Aspect Ratio for the plain wings.

FIG. 5.

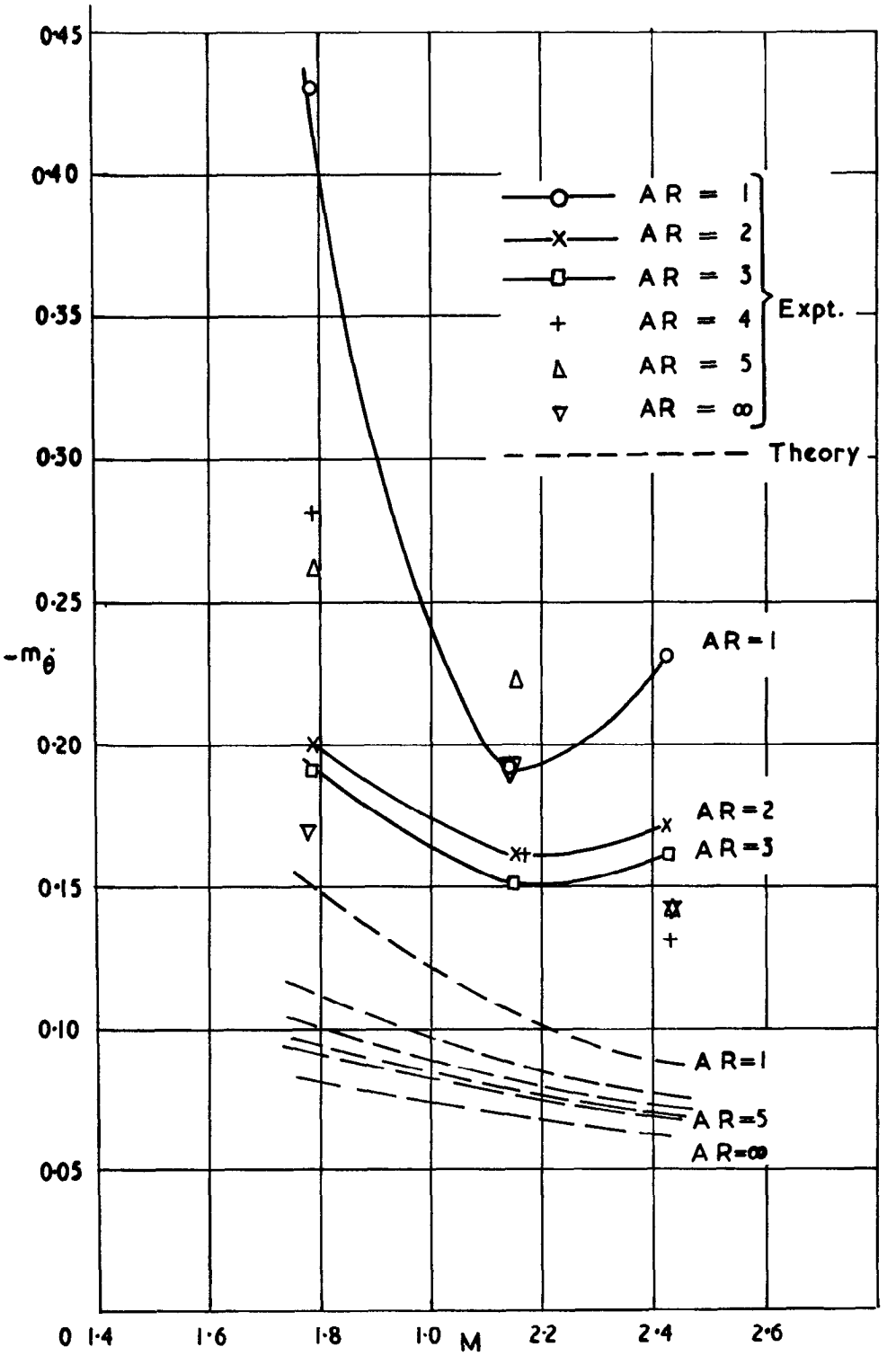

Variation of $-m_{\dot{\theta}}$ with Mach number for the plain wings.

FIG. 6.

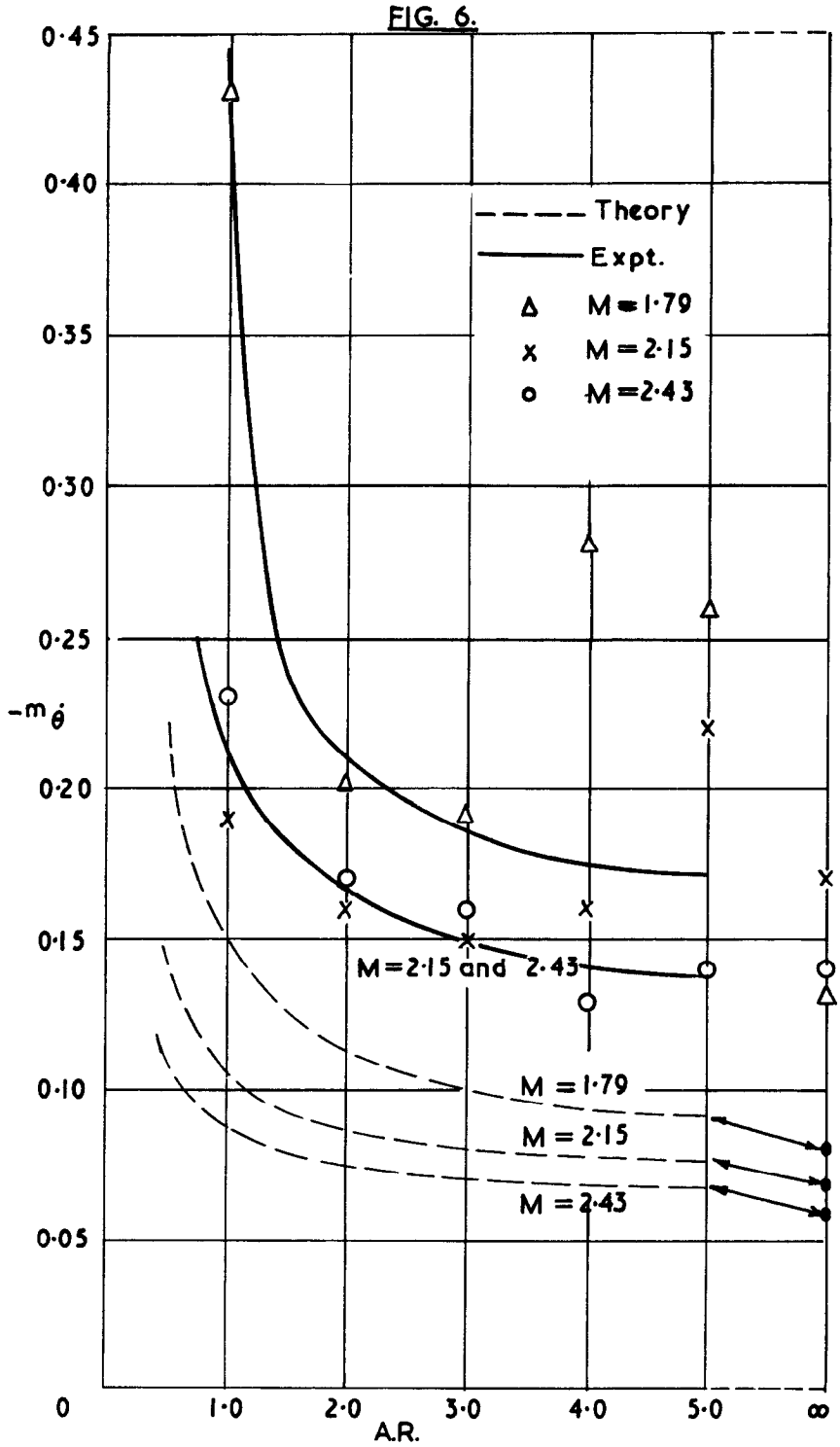

Variation of $-m_{\dot{\theta}}$ with Aspect Ratio for the plain wings.

FIG. 7(a - e)

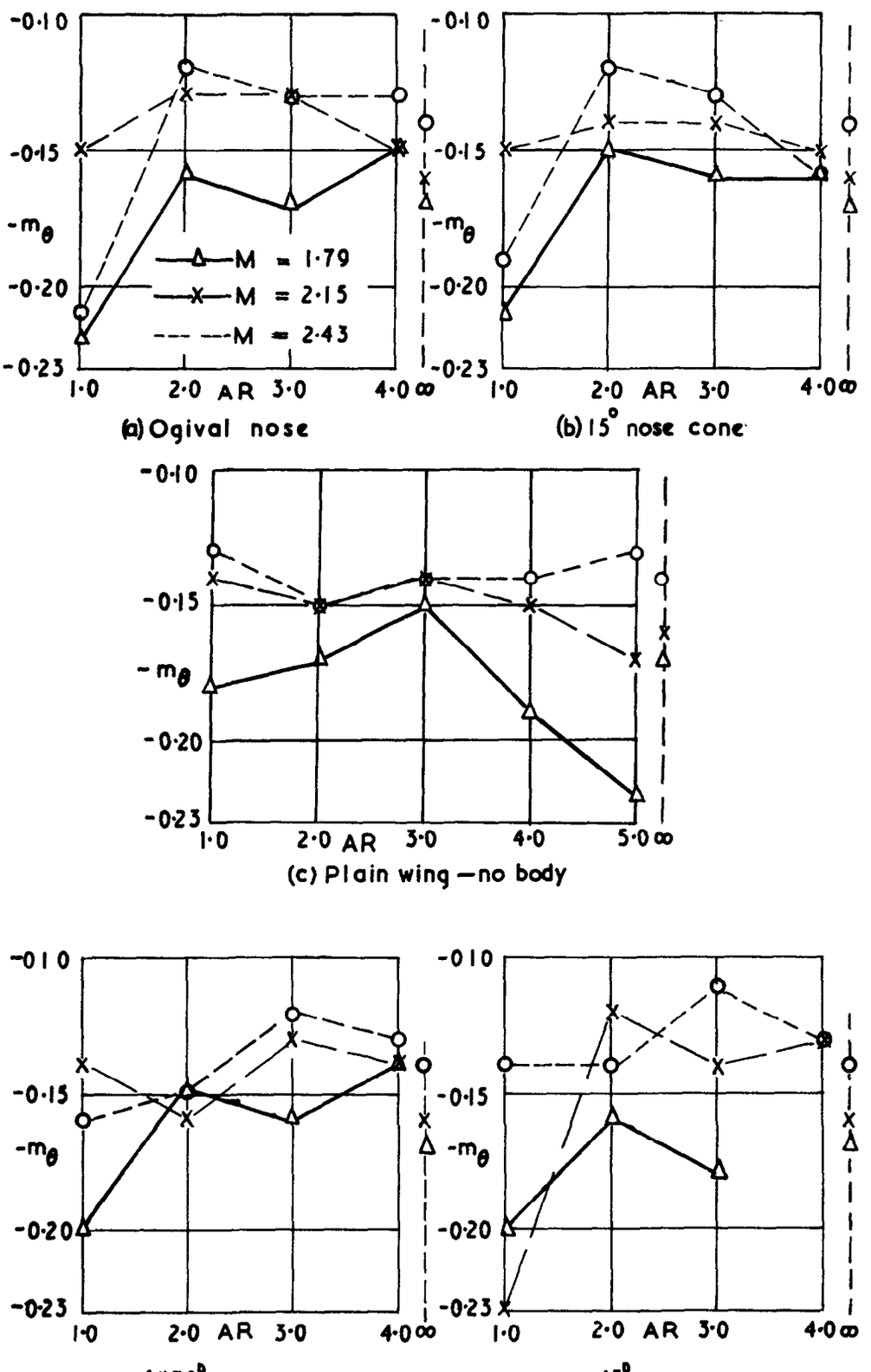

Variation of $-m_\theta$ with aspect ratio.

FIG.8.a-d.

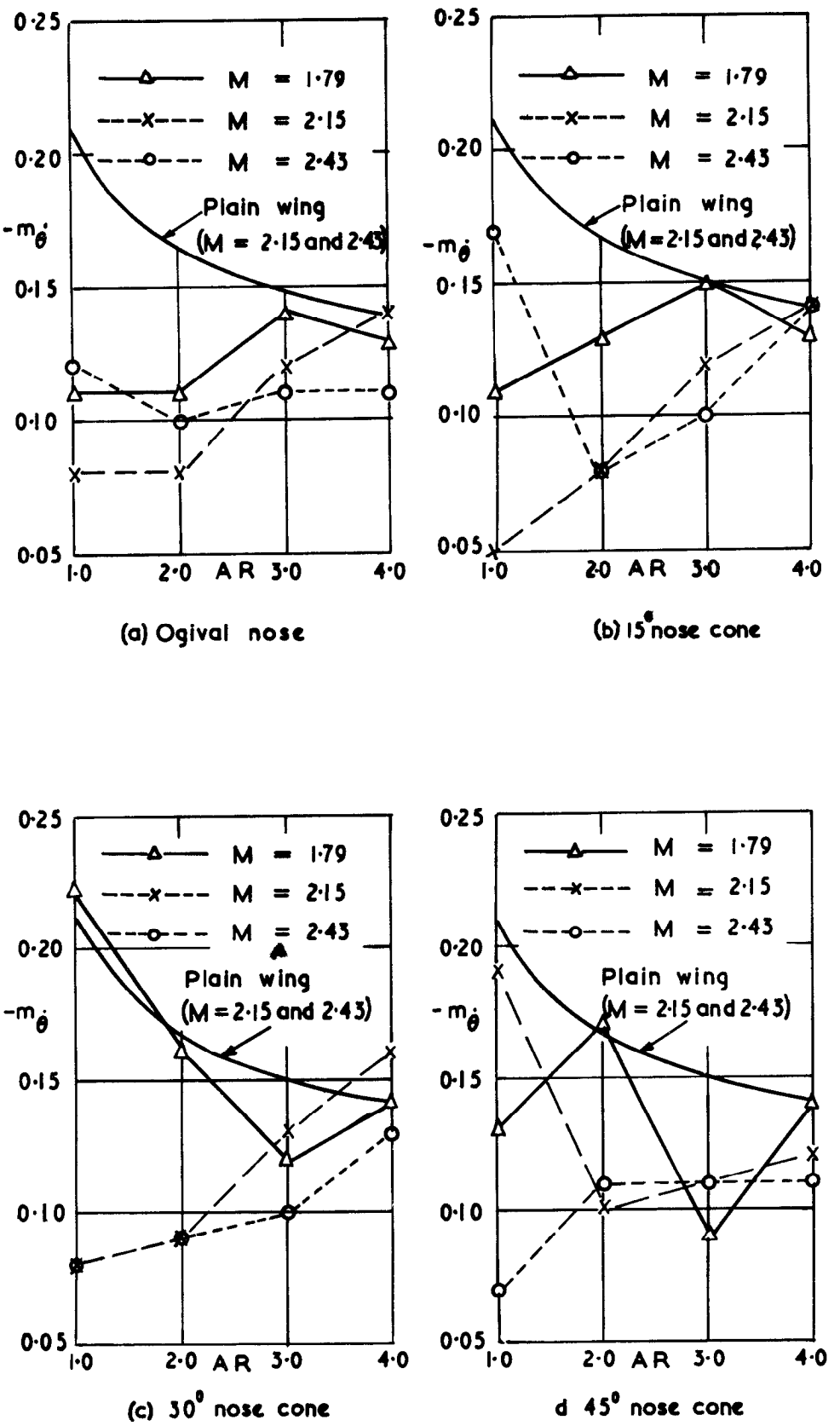

Variation of $-m_{\dot{\theta}}$ with Aspect Ratio for wings adjacent to bodies with various nose shapes.

A.R.C. C.P. No.594. March, 1961.

Scruton, C., Woodgate, L., Lapworth, K. C. and
Maybrey, J. F. M. Nat Phys. Lab.

MEASUREMENTS OF THE PITCHING MOMENT DERIVATIVES FOR RIGID WINGS OF RECTANGULAR PLAN FORM OSCILLATING ABOUT THE MID-CHORD AXIS IN SUPERSONIC FLOW

Results are given of the measurements of pitching moment derivatives for wings of rectangular planform of aspect ratio from 1 to 5 oscillating in supersonic flow. The influence of a body with various nose shapes was also investigated. It was found that the general trend of the variation of the derivatives with aspect ratio was predicted by theory.

A.R.C. C.P. No.594. March, 1961.

Scruton, C., Woodgate, L., Lapworth, K. C. and
Maybrey, J. F. M. Nat. Phys. Lab.

MEASUREMENTS OF THE PITCHING MOMENT DERIVATIVES FOR RIGID WINGS OF RECTANGULAR PLAN FORM OSCILLATING ABOUT THE MID-CHORD AXIS IN SUPERSONIC FLOW

Results are given of the measurements of pitching moment derivatives for wings of rectangular planform of aspect ratio from 1 to 5 oscillating in supersonic flow. The influence of a body with various nose shapes was also investigated. It was found that the general trend of the variation of the derivatives with aspect ratio was predicted by theory.

A.R.C. C.P. No.594. March, 1961.

Scruton, C., Woodgate, L., Lapworth, K. C. and
Maybrey, J. F. M. Nat. Phys. Lab.

MEASUREMENTS OF THE PITCHING MOMENT DERIVATIVES FOR RIGID WINGS OF RECTANGULAR PLAN FORM OSCILLATING ABOUT THE MID-CHORD AXIS IN SUPERSONIC FLOW

Results are given of the measurements of pitching moment derivatives for wings of rectangular planform of aspect ratio from 1 to 5 oscillating in supersonic flow. The influence of a body with various nose shapes was also investigated. It was found that the general trend of the variation of the derivatives with aspect ratio was predicted by theory.

Printed and published by
HER MAJESTY'S STATIONERY OFFICE
To be purchased from
York House, Kingsway, London, W.C.2
423 Oxford Street, London W.1
13A Castle Street, Edinburgh 2
109 St. Mary Street, Cardiff
39 King Street, Manchester 2
50 Fairfax Street, Bristol 1
35 Smallbrook, Ringway, Birmingham 5
80 Chichester Street, Belfast 1
or through any bookseller

Printed in England

S.O. Code No. 23-9012-94